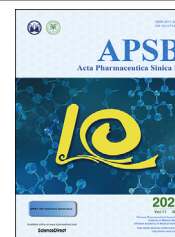




Chinese Pharmaceutical Association
Institute of Materia Medica, Chinese Academy of Medical Sciences

Acta Pharmaceutica Sinica B

www.elsevier.com/locate/apsb
www.sciencedirect.com



ORIGINAL ARTICLE

Preclinical efficacy against acute myeloid leukaemia of SH1573, a novel mutant IDH2 inhibitor approved for clinical trials in China



Zhiqiang Wang^{a,†}, Zhibo Zhang^{a,†}, Yong Li^{b,†}, Li Sun^a, Dezhen Peng^a, Danyu Du^a, Xian Zhang^c, Luwei Han^c, Liwen Zhao^c, Ligong Lu^b, Hongzhi Du^{d,*}, Shengtao Yuan^{a,*}, Meixiao Zhan^{b,*}

^aJiangsu Key Laboratory of Drug Screening, China Pharmaceutical University, Nanjing 210003, China

^bZhuhai Interventional Medical Center, Zhuhai Precision Medical Center, Zhuhai People's Hospital, Zhuhai Hospital Affiliated with Jinan University, Jinan University, Zhuhai 519000, China

^cSanhome Pharmaceutical Co., Ltd., Nanjing 210000, China

^dSchool of Pharmacy, Hubei University of Chinese Medicine, Wuhan 430065, China

Received 11 January 2021; received in revised form 2 February 2021; accepted 7 February 2021

KEY WORDS

Acute myeloid leukaemia;
Tumor metabolism;
Mutant isocitrate dehydrogenase 2 (mIDH2);
mIDH2 inhibitor;
SH1573;
2-Hydroxyglutarate;
Differentiation;

Abstract Acute myeloid leukaemia (AML) is the most common form of acute leukaemia in adults, with increasing incidence with age and a generally poor prognosis. Almost 20% of AML patients express mutant isocitrate dehydrogenase 2 (mIDH2), which leads to the accumulation of the carcinogenic metabolite 2-hydroxyglutarate (2-HG), resulting in poor prognosis. Thus, global institutions have been working to develop mIDH2 inhibitors. SH1573 is a novel mIDH2 inhibitor that we independently designed and synthesised. We have conducted a comprehensive study on its pharmacodynamics, pharmacokinetics and safety. First, SH1573 exhibited a strong selective inhibition of mIDH2 R140Q protein, which could effectively reduce the production of 2-HG in cell lines, serum and tumors of an animal model. It could also promote the differentiation of mutant AML cell lines and granulocytes in PDX models. Then, it was

Abbreviations: 2-HG, 2-hydroxyglutaric acid; ADME, absorption, distribution, metabolism and excretion; AG-221, enasidenib; AML, acute myeloid leukemia; AUC, area under the curve; BCRP, breast cancer resistance protein; CDX, cell-line-derived xenograft; CYP, cytochrome P450; EPO, erythropoietin; IC₅₀, half maximal inhibitory concentration; α -KG, α -ketoglutaric acid; LC–MS/MS, liquid chromatography–tandem mass spectrometry; MDR1, multidrug resistance protein 1; mIDH2, mutant isocitrate dehydrogenase; OAT, organic anion transporter; OATP, organic anion transporting polypeptide; OCT, organ cation transporter; P_{app} , apparent permeability coefficient; PD, pharmacodynamics; PDX, patient-derived tumor xenograft; PK, pharmacokinetics.

*Corresponding authors.

E-mail addresses: dhz3163@hbtcu.edu.cn (Hongzhi Du), yuanst@cpu.edu.cn (Shengtao Yuan), zhanmeixiao1987@126.com (Meixiao Zhan).

†These authors made equal contributions to this work.

Peer review under responsibility of Chinese Pharmaceutical Association and Institute of Materia Medica, Chinese Academy of Medical Sciences.

<https://doi.org/10.1016/j.apsb.2021.03.005>

2211-3835 © 2021 Chinese Pharmaceutical Association and Institute of Materia Medica, Chinese Academy of Medical Sciences. Production and hosting by Elsevier B.V. This is an open access article under the CC BY-NC-ND license (<http://creativecommons.org/licenses/by-nc-nd/4.0/>).

Preclinical efficacy

confirmed that SH1573 possessed characteristics of high bioavailability, good metabolic stability and wide tissue distribution. Finally, toxicological data showed that SH1573 had no effects on the respiratory system, cardiovascular system and nervous system, and was genetically safe. This research successfully promoted the approval of SH1573 for clinical trials (CTR20200247). All experiments demonstrated that, as a potential drug against mIDH2 R140Q acute myeloid leukaemia, SH1573 was effective and safe.

© 2021 Chinese Pharmaceutical Association and Institute of Materia Medica, Chinese Academy of Medical Sciences. Production and hosting by Elsevier B.V. This is an open access article under the CC BY-NC-ND license (<http://creativecommons.org/licenses/by-nc-nd/4.0/>).

1. Introduction

Since Hanahan and Weinberg¹ summarised the characteristics of deregulating metabolism in tumor cells, the abnormal metabolism of tumors has attracted increasing attention from scientists. Mutations in the metabolic genes contribute to the initiation, development, and maintenance of tumors, so targeting tumor metabolism has become a hot spot for anti-tumor drug development^{2–4}. In particular, the isocitrate dehydrogenases (IDHs) are a critical enzyme family in the Krebs cycle, including three enzymes (IDH1, IDH2, and IDH3). IDH could catalyse the conversion of isocitrate to α -ketoglutarate (α -KG) using divalent magnesium ion and NADP⁺ (or NAD⁺) as cofactors⁵. IDH mutations have been frequently found in IDH1 R132H and IDH1 R132C or IDH2 R140Q and IDH2 R172K, which located in the catalytic pocket of these enzymes. The mutations are loss- and gain-of-function mutations, which convert α -KG to 2-HG^{6,7}. High intracellular 2-HG could competitively inhibit α -KG-dependent dioxygenase, resulting in hypermethylation of histone and DNA^{8,9}. The change of methylation status could decrease expression of genes relative to cell differentiation¹⁰. Therefore, IDH mutations are considered closely related to the genesis and development of tumors.

In AML, approximately 20% of patients carry *IDH2* mutations, among which R140Q accounts for about 80% of the total mIDH2 protein, and R172K accounts for about 20%^{11,12}. Importantly, increasing researches have shown that *IDH* mutations are indicators of prognosis^{13,14}. As clinical observation¹⁵, in AML patients, mIDH2 R172K indicates a poor prognosis, but mIDH2 R140Q often indicates a good prognosis. However, the prognostic impact of R140Q may be dependent on co-occurring mutations. For instance, AML patients harboring the mIDH2 R140Q in conjunction with *NMP1* gene mutation in have been identified as having a worse overall survival¹⁶. In other words, mIDH2 R140Q also maybe result in a poor prognosis. Actually, 2-HG levels in patients with mIDH2 R140Q are 10 times higher than those in IDH wild-type patients¹⁷. As reported¹⁸, adding 2-HG in TF-1 cells could inhibit the normal differentiation of hematopoietic cells and promote tumor cell proliferation. Previous studies have also suggested that inhibiting the activity of the mIDH2 enzyme could reduce the concentration of 2-HG and restore the differentiation ability of leukaemia cells. Enasidenib (AG-221), an inhibitor of mIDH2, could differentiate primary progenitor cells into mature granulocytes¹⁹. Therefore, for AML patients carrying *IDH2* mutations, inhibiting the function of IDH2 mutant enzymes to reduce 2-HG level could lead to considerable therapeutic effect^{20,21}. Since the U.S. Food and Drug Administration (FDA) approved AG-221 to treat relapsed and refractory

adult AML patients with mIDH2 in 2017, global pharmaceutical companies have been committed to the development of mIDH2 inhibitors²². Currently, AG-221 and ivosidenib have been approved for marketing, while HMPL-306 and AG-881 have been approved for clinical trials^{23,24}. Obviously, mIDH2 is an effective target for the treatment of AML.

In this study, we conducted a comprehensive drug evaluation on SH1573. First, we tested the effect of SH1573 on mIDH2 inhibition, 2HG reduction, and cell differentiation induction *in vitro* and *in vivo*. Then, we analyzed the absorption, distribution, metabolism, and excretion (ADME) of SH1573 in Sprague–Dawley rats and cynomolgus monkeys. Moreover, we evaluated the safety of SH1573 and explored the no observed adverse effect level as the reference dose for clinical trials. All experiments confirmed that SH1573 was a novel, effective, and safe mIDH2 R140Q inhibitor. As a result, SH1573 has been approved for clinical trials in China (CTR20200247), and our study provides a reference for the development of trials. In brief, it is hopeful that SH1573 will become a self-developed and successfully marketed drug targeting mIDH2 R140Q in China to serve the clinic.

2. Materials and methods

2.1. Chemicals and reagents

SH1573 (SH1573-20170708) was synthesized and provided by Sanhome Pharmaceutical Co., Ltd. (Nanjing, China). Other chemicals and reagents can be found in Supporting Information (Appendix B).

2.2. Cell lines and animals

The source, breeding conditions of all cell lines and animals in this experiment can be found in Supporting Information (Appendix B). Ethical approvals for the rat experiments were obtained from the Animal Ethics Committee of China Pharmaceutical University (Nanjing, China). Ethical approvals for the monkey experiments were obtained from the Pharmaron Co., Ltd. (Beijing, China) and Covance Pharmaceutical R&D Co., Ltd. (Shanghai, China).

2.3. Molecular docking

The crystal structure of mIDH2 was searched on the RCSB Protein Data Bank (ID: 5I96). The detailed process for molecular docking can be found in Supporting Information (Appendix B).

2.4. Enzyme activity analysis

The detailed methods for inhibitory effects assay on IDHs protein and kinase profiling assay can be seen in Supporting Information (Appendix B).

2.5. Pharmacodynamic (PD) experiment in cell

The detailed methods for 2-HG reducing assay, cell activity assay and cell differentiation assay can be seen in Supporting Information (Appendix B).

2.6. PD experiment in vivo

The detailed methods for subcutaneous CDX model, PDX model can be seen in Supporting Information (Appendix B).

2.7. Pharmacokinetic (PK) analysis in vitro

The detailed methods for two-way penetration experiment, protein binding rate experiment and liver microsomal biotransformation experiment can be seen in Supporting Information (Appendix B).

2.8. PK analysis in vivo

The detailed methods for absorption experiment of rats and monkeys, tissue distribution experiment of rats, drug excretion experiment and biotransformation experiment can be seen in Supporting Information (Appendix B).

2.9. Drug–drug interaction analysis

The detailed methods for inhibitory effects analysis of SH1573 to cytochrome P450 (CYPs), metabolic stability analysis of SH1573 in CYPs, inhibitory effects analysis of SH1573 on transporters and uptake ratio analysis of transporters on SH1573 can be seen in Supporting Information (Appendix B).

2.10. Safety evaluation of SH1573

The detailed methods for respiratory safety assay, central nervous system safety assay, cardiovascular system safety assay and potassium channel assay can be seen in Supporting Information (Appendix B).

2.11. Toxicity analysis of SH1573

The detailed methods for acute toxicity assay and repeated administration toxicity assay can be seen in Supporting Information (Appendix B).

2.12. Genotoxicity analysis of SH1573

The detailed methods for Ames test, rat micronucleus test and chromosome aberration test can be seen in Supporting Information (Appendix B).

2.13. Statistical analysis

All data were expressed as mean \pm standard deviation (SD) and two-sample *t*-test was used to compare the statistical differences between two independent counting samples. Kaplan–Meier

survival curve was used for survival analysis and logRank test was used for analysis. In the part of toxicity analysis, quantitative data results were statistically analyzed using One-Way ANOVA between groups and Dunnett's multiple comparison method was used. When the size of the group was less than 3, no further statistical analysis will be done. In chromosome aberrant test, Fisher's exact test was used. All data were analyzed using Graphpad Prism 7.0 and two-sided $P < 0.05$ was considered a significant difference.

3. Results

3.1. SH1573 selectively inhibited the activity of mIDH2 R140Q

SH1573 is a compound with a new structure designed to inhibit mIDH2 R140Q (Fig. 1A); its detailed information can be seen in Supporting Information Fig. S1A and S1B. First, molecular docking was carried out between SH1573 and mIDH2 R140Q (PDB ID:5I96) to understand the molecular biology. Unlike the binding site of AG-221, SH1573 bound to another allosteric site (Fig. 1B), and the detailed binding sites are shown in Fig. 1C. Thus, it could be seen that SH1573 was a potential novel mIDH2 inhibitor. Then, we carried out an enzyme activity assay to explore the direct impact of SH1573 on different enzymes. The results show that SH1573 had a strong inhibitory effect on mIDH2 R140Q and R172K, with a half maximal inhibitory concentration (IC₅₀) of 4.78 and 14.05 nmol/L, while its IC₅₀ for wild-type IDH2 was 196.2 nmol/L (Fig. 1D–F). Moreover, inhibitory activity of SH1573 against mIDH1 R132H and wild-type IDH1 had not been observed at the concentration of 100 μ mol/L (Fig. S1C and Fig. 1G). To further verify its targetability, SH1573 was applied to a series of hotspot enzymes in the human body. It was found that at a concentration of 10 μ mol/L, SH1573 had no significant effect on the relative activities of 23 enzymes (Fig. 1H). Undoubtedly, SH1573 could selectively and significantly inhibit mIDH2 R140Q.

3.2. SH1573 decreased 2-HG level and promoted cell differentiation in vitro

It is well known that the production of 2-HG and blocked differentiation are important features of mIDH2 mutation cells. Therefore, we initially confirmed that SH1573 dose-dependently inhibited the production of 2-HG in TF-1 (mIDH2 R140Q) cells, with an IC₅₀ value of 25.3 nmol/L (Fig. 2A). The IC₅₀ values of SH1573 for inhibiting 2-HG production in U87-MG (mIDH2 R140Q) cells, U87-MG (mIDH2 R172K) and SW1353 (mIDH2 R172S) cells were 0.27, 0.053 and 4.51 μ mol/L, respectively (Fig. 2B and Fig. S1E). Because SH1573 did not inhibit the proliferation of TF-1 cells at IC₅₀ concentration on 2-HG (Fig. 2C and D), the inhibition of 2-HG production was just *via* inhibiting the activity of the IDH2 R140Q enzyme. Obviously, SH1573 had the strongest effect on R140Q mutation, and R140Q had a wider range in patients. Therefore, R140Q mutation became the focus of follow-up experimental investigation.

Next, we used erythropoietin (EPO) to explore the effect of SH-1573 on cell differentiation²⁵. Wild-type TF-1 cells could differentiate into red blood cells under EPO stimulation, but TF-1 (mIDH2 R140Q) cells did not. When TF-1 (mIDH2 R140Q) cells were incubated with 1 μ mol/L SH1573 under stimulation of EPO, red colour of the cells and increased expression of haemoglobin at

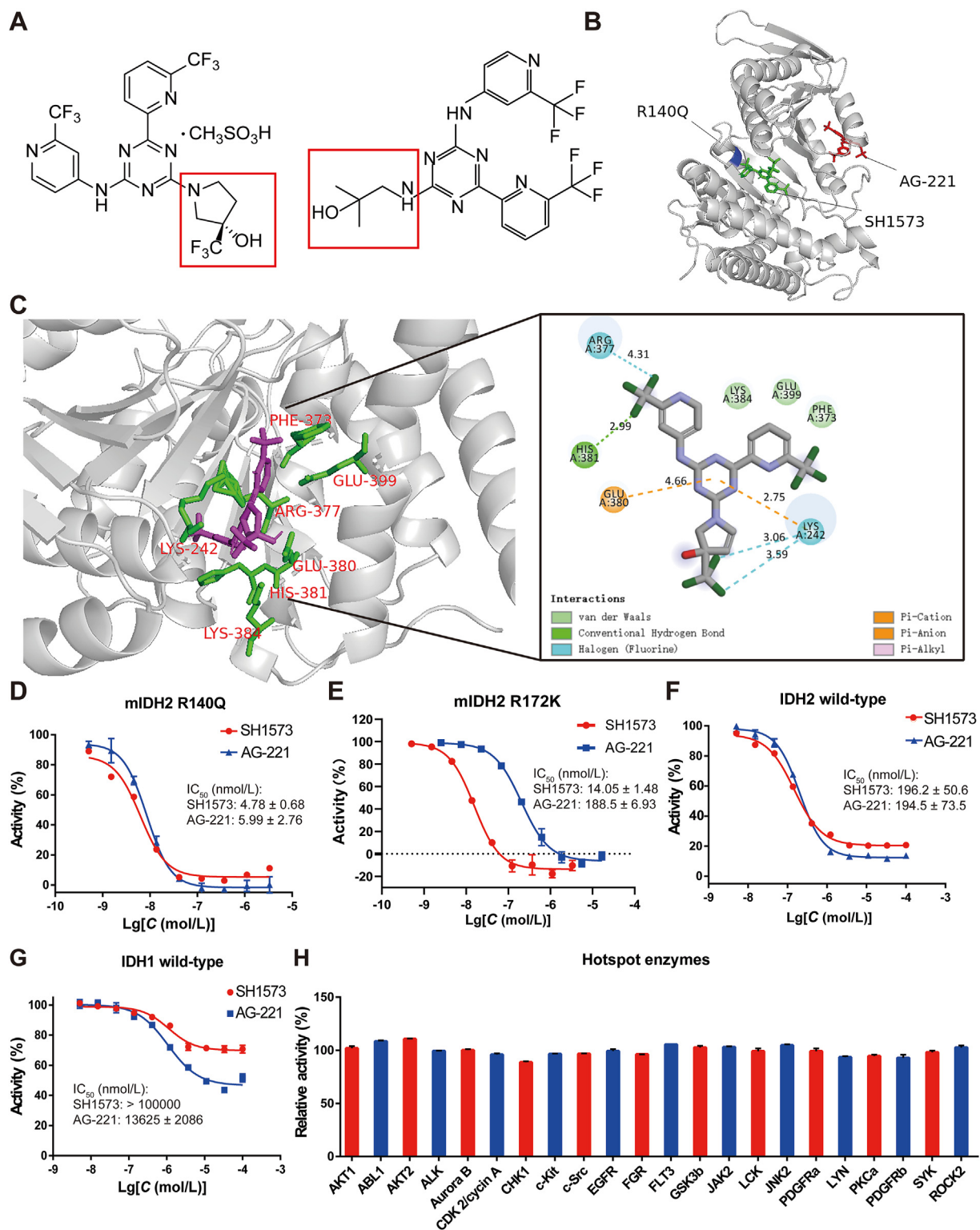


Figure 1 The enzyme activity assay of SH1573. (A) Chemical structure of SH1573. (B) and (C) The molecular dynamics were evaluated using GROMACS and the ligand with lowest energy and most favorable orientation was selected. (D)–(H) The directly inhibitory effects of SH1573 and AG-221 on mIDH2 R140Q/R172K, wild-type IDH 1/2 and 23 types enzymes (AKT1, ABL1, AKT2, ALK, Aurora B, CDK 2/cyclin A, CHK1, c-Kit, c-Src, EGFR, FGR, FLT3, GSK3b, JAK2, LCK, JNK2, PDGFRa, LYN, PKCa, PDGFRb, SYK, and ROCK2). All data are expressed as mean ± SD ($n = 3$).

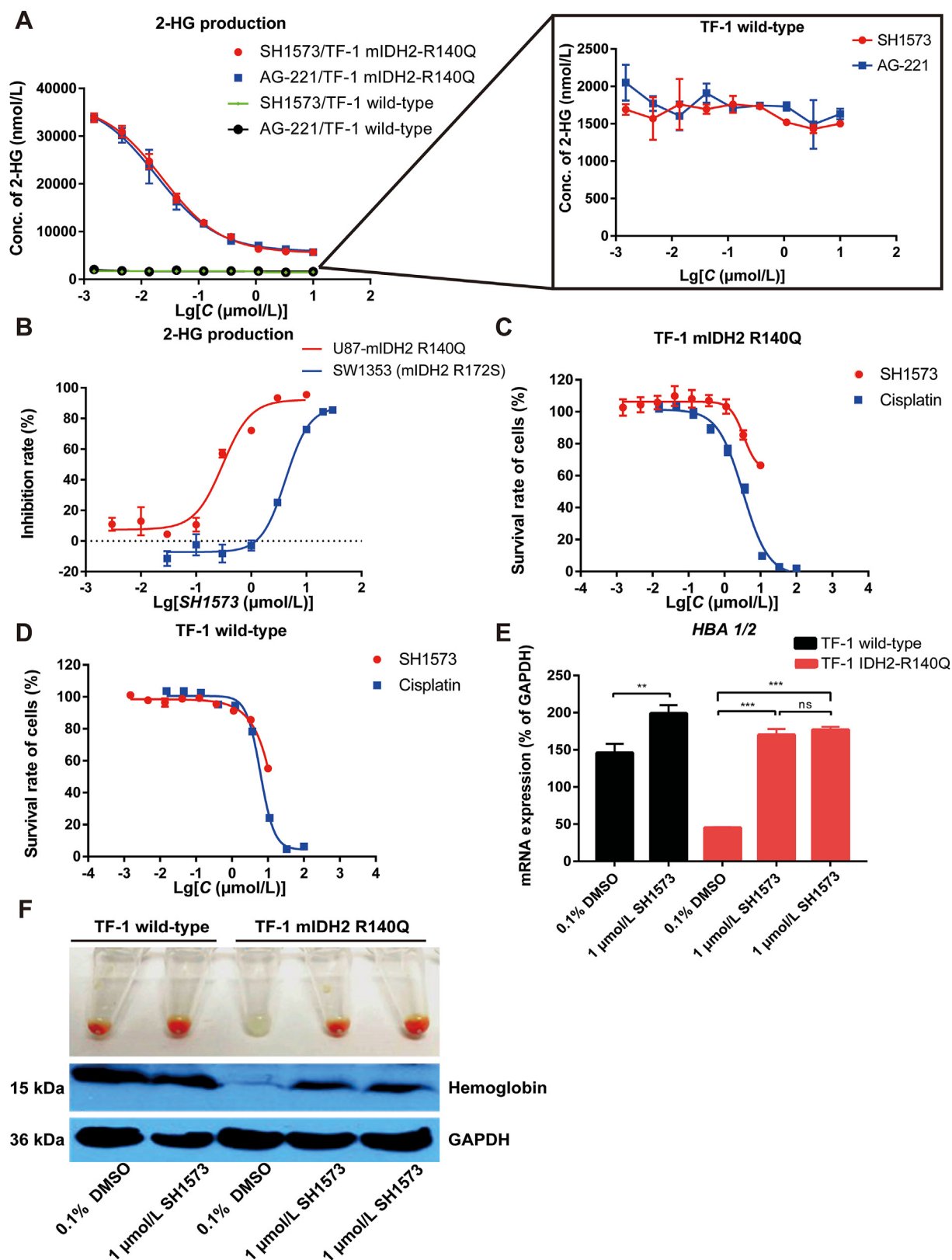


Figure 2 The effects of SH1573 *in vitro*. (A) and (B) SH1573 reduced the production of 2-HG in TF-1 (mIDH2 R140Q), U87 (mIDH2 R140Q) and SW1353. (C) and (D) SH1573 had moderate proliferation inhibition on TF-1 (wild-type) and TF-1 (mIDH2 R140Q). (E) and (F) SH1573 reversed the cell differentiation by promote the mRNA and protein expression of hemoglobin. All data are expressed as mean \pm SD ($n = 3$); * $P < 0.05$, ** $P < 0.01$, *** $P < 0.001$, ns: no significant difference (E).

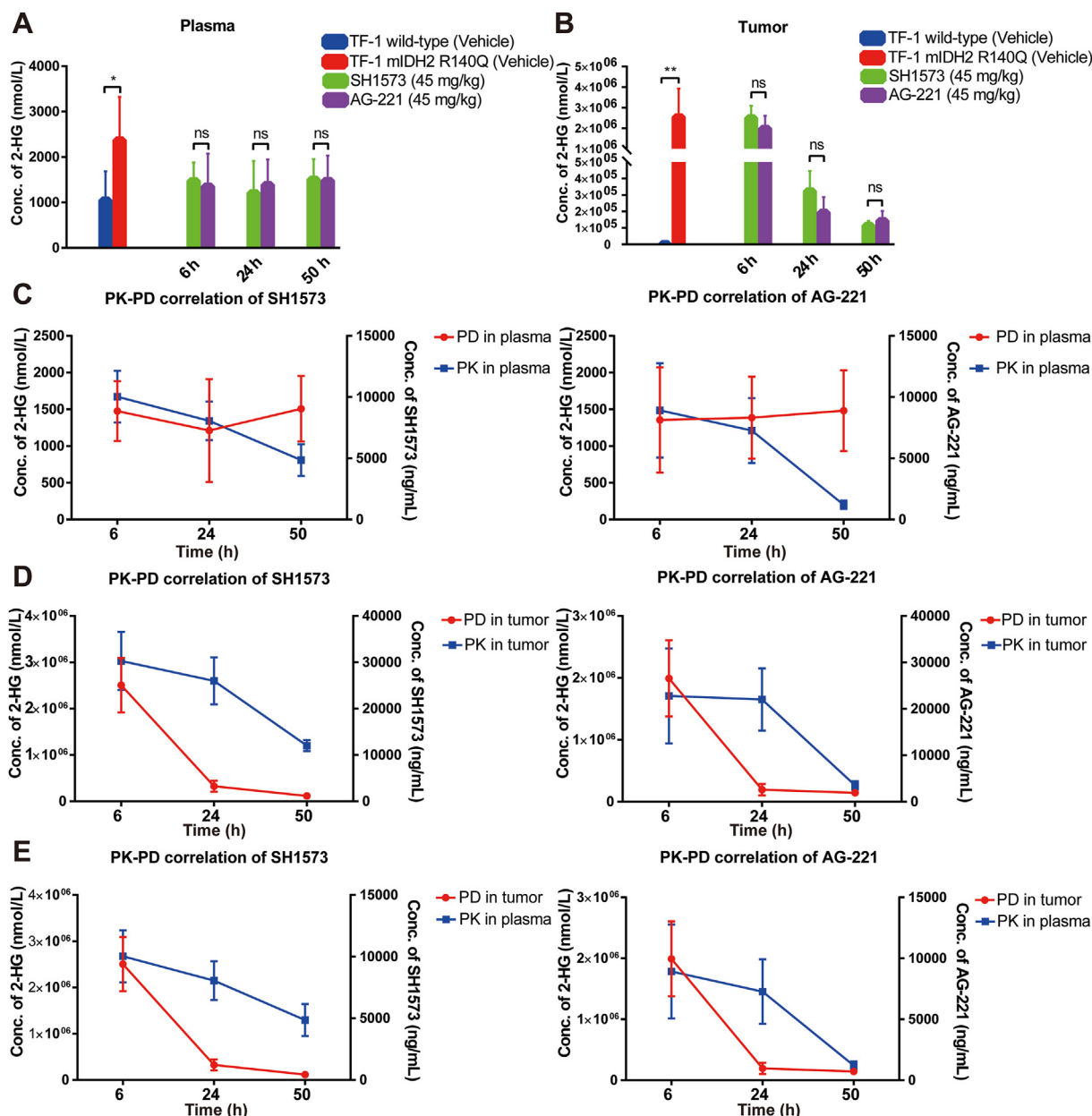


Figure 3 The PK–PD analysis of SH1573 in subcutaneous xenograft model. (A) and (B) Mice were inoculated TF-1 (mIDH2 R140Q) cells subcutaneously and treated for once with vehicle ($n = 6$), 45 mg/kg SH1573 i.g. ($n = 18$) or 45 mg/kg AG-221 i.g. ($n = 18$), and LC–MS/MS was used to analysis the concentration of 2-HG, SH1573 and AG-221 in plasma or tumor. SH1573 and AG-221 reduced the 2-HG level in plasma and tumor after 6, 24 and 50 h. (C)–(E) The PK–PD analysis of SH1573 or AG-221 in plasma, tumor and in both of them ($n = 6$). All data are expressed as mean \pm SD; * $P < 0.05$; ** $P < 0.01$, ns: no significant difference (A and B).

the gene and protein levels were observed, indicating that the ability to differentiate into red blood cells was restored²⁶ (Fig. 2E and F). These results show that SH1573 reduced the level of 2-HG and promote cell differentiation *in vitro*.

3.3. PK–PD analysis of SH1573 in a subcutaneous CDX model

To investigate the PK–PD progress of SH1573, preliminarily, *in vivo*, TF-1 (mIDH2 R140Q) cells were used to construct a subcutaneous CDX model. As expected, the levels of 2-HG in the plasma and tumors of mice inoculated with TF-1 (mIDH2 R140Q) cells were higher than that of mice inoculated with TF-1 (wild

type) cells (Fig. 3A and B). After a single administration of SH1573 (45 mg/kg), the level of 2-HG in plasma remained low from 6 to 50 h (Fig. 3C). SH1573 (45 mg/kg) reduced intratumoral 2-HG levels by 1.9%, 87.4% and 95.7% after administration for 6, 24 or 50 h, respectively (Fig. 3D). Although the corresponding plasma–drug concentration was high at 6 h, the 2-HG level in the tumor did not decrease significantly. By contrast, the plasma–drug concentration was in a downward trend from 24 to 50 h, the 2-HG concentration in plasma remained at a low level and the 2-HG level in the tumor continued to decrease (Fig. 3E). These results indicate that SH1573 continuously reduced 2HG levels and enter the tumor tissue.

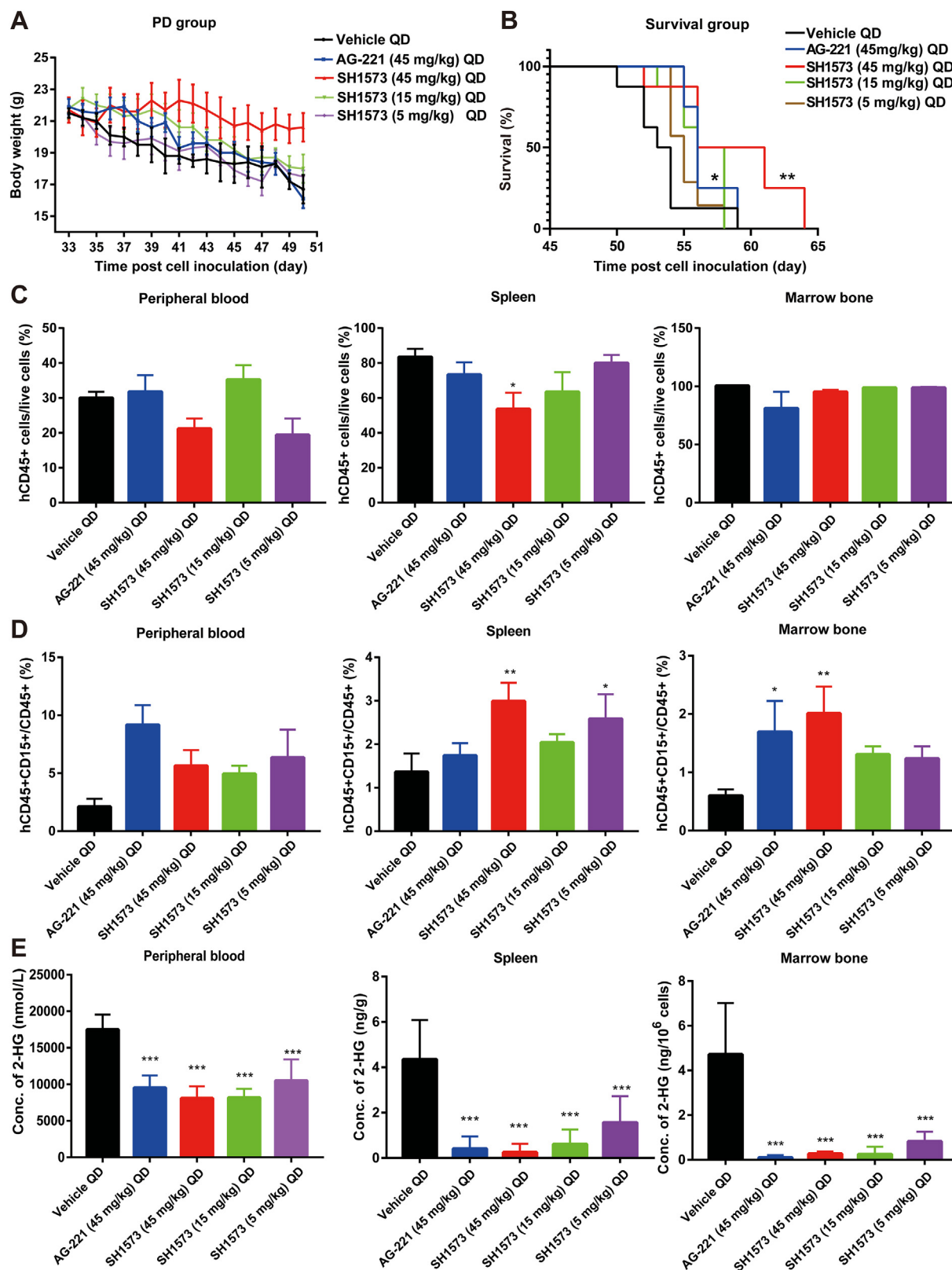


Figure 4 The anti-tumor effects of SH1573 in PDX model. (A) and (B) Mice were injected primary AML cell obtained from a patient *via* tail vein and treated with vehicle QD *p.o.*, 45 mg/kg AG-221 QD *p.o.*, 5 mg/kg SH1573 QD *p.o.*, 15 mg/kg SH1573 QD *p.o.* or 5 mg/kg SH1573 QD *p.o.* Six mice in each group was for PD analysis and nine mice was for survival analysis. The SH1573 could maintain the body weight ($n = 6$) and prolong survival time of mice ($n = 9$). (C) In peripheral blood and marrow bone, SH1573 did not significantly reduce tumor burden ($n = 6$). (D) SH1573 promote cell differentiation ($n = 6$). (E) SH1573 reduced 2-HG level ($n = 6$). Data are expressed as mean \pm SD; * $P < 0.05$, ** $P < 0.01$, *** $P < 0.001$ versus Vehicle QD group (B–E).

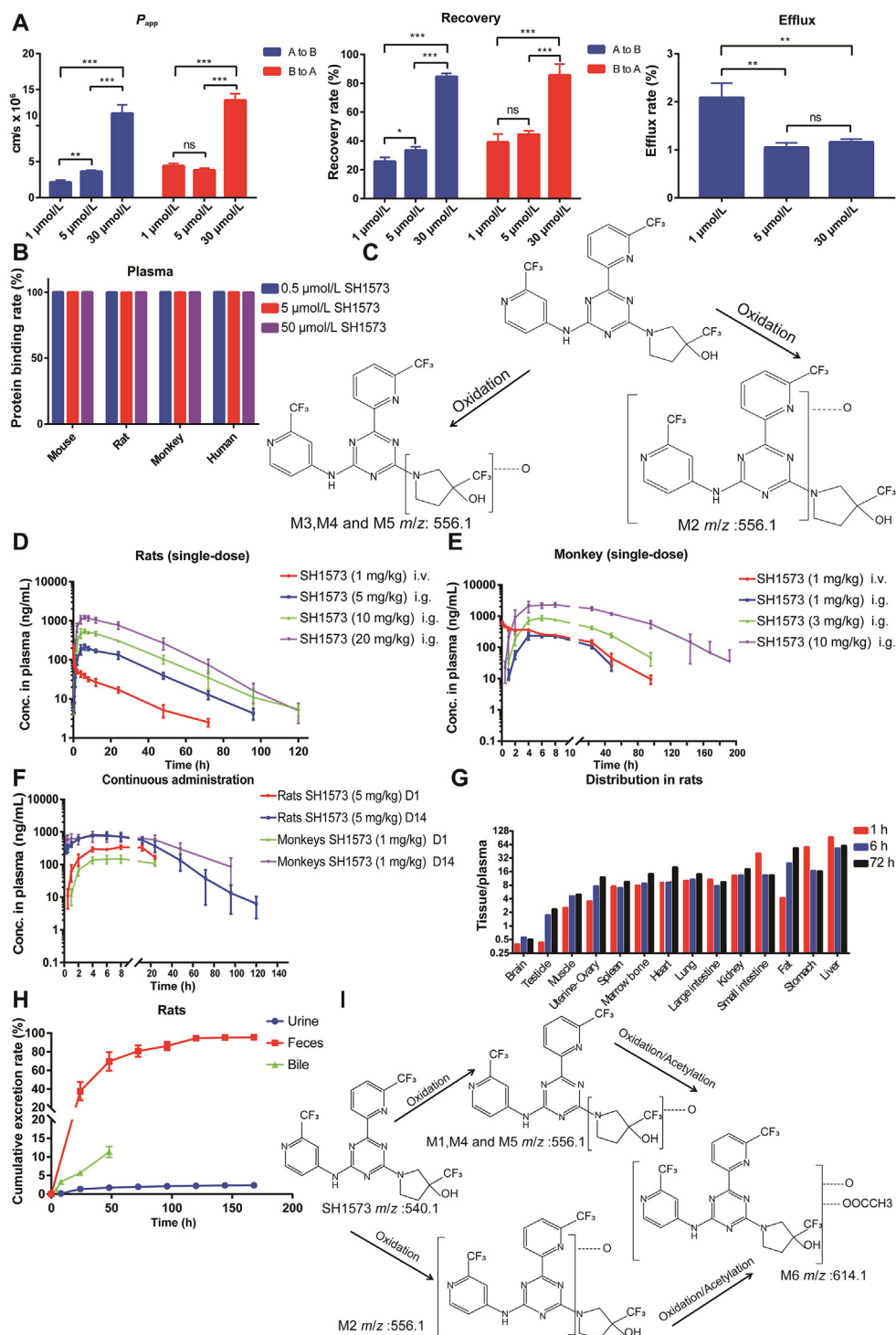


Figure 5 PK process of SH1573. (A) The P_{app} , recovery rate and efflux rate of SH1573 detected by Caco-2 model ($n = 3$). (B) The binding rate of SH1573 to plasma protein of mouse, rat, monkey and human ($n = 3$). (C) Four metabolites of SH1573 in liver microsomes detected by LC–MS/MS. (D) SD rats were treated for once with 1 mg/kg SH1573 i.v., 5 mg/kg SH1573 i.g., 10 mg/kg SH1573 i.g. or 20 mg/kg SH1573 i.g., and plasma drug concentration was detected by LC–MS/MS ($n = 6$). (E) Monkeys were treated for once with 1 mg/kg SH1573 i.v., 1 mg/kg SH1573 i.g., 3 mg/kg SH1573 i.g. or 10 mg/kg SH1573 i.g., and plasma drug concentration was detected by LC–MS/MS ($n = 6$). (F) Rats and monkey were treated for 14 days with 5 or 1 mg/kg SH1573 i.g., respectively. Plasma drug concentration on Day 1 and Day 14 was detected by LC–MS/MS ($n = 6$). (G) The drug distribution in rats treated with 10 mg/kg SH1573 i.g. was detected by LC–MS/MS ($n = 18$). (H) The [¹⁴C] SH1573 in urine, feces and bile of rats was traced by HPLC radio chromatography ($n = 18$). (I) Five metabolites were detected in plasma of monkey using LC–MS/MS ($n = 6$). Data are expressed as mean ± SD; * $P < 0.05$, ** $P < 0.01$, *** $P < 0.001$, ns: no significant difference (A).

3.4. SH1573 exhibited anti-tumor effects in the PDX model

Because AML is not a solid tumor, the PDX model was used to evaluate the anti-tumor effects of SH1573 accurately^{27,28}. After administration for 18 days, 45 mg/kg SH1573 could maintain the body weight in a certain extent (Fig. 4A). Meanwhile, at a dose of 45 mg/kg, both AG-221 and SH1573 could significantly prolong the survival period of PDX-bearing mice, and SH1573 had a better effect (Fig. 4B). Although each dose of SH1573 did not reduce the tumor burden in the peripheral blood and bone marrow (Fig. 4C), they increased the proportion of CD15⁺ cells. Compared with the vehicle group, each dose of SH1573 also moderately increased the proportion of differentiated tumor cells (hCD45⁺ hCD15⁺) in the terminal spleen and bone marrow (Fig. 4D). It was suggested that SH1573 could promote the differentiation of AML cells in a dose-dependent manner²⁹. In addition, each dose of SH1573 could dose-dependently reduce the level of 2-HG in peripheral blood, spleen and bone marrow (Fig. 4E). Therefore, these results suggest SH1573 exhibited anti-tumor effects *via* reducing the level of 2-HG and promoting cell differentiation *in vivo*.

3.5. PK analysis of SH1573 *in vitro*

Satisfactory ADME processing of drugs is key to ensuring clinical efficacy, so we performed PK analysis *in vitro* after PD analysis. The Caco-2 cell model showed that the apparent permeability coefficient (P_{app}) of SH1573 from top to bottom was 2.14×10^6 – 11.7×10^6 cm/s in the concentration range of 1–30 μ mol/L, and that from bottom to top was 3.80×10^6 – 13.5×10^6 cm/s (Fig. 5A). The efflux rate of 1 μ mol/L SH1573 was 2.09 and decreased with increasing concentration of SH1573, indicating that SH1573 may be a weak substrate of the efflux transporter^{30,31} (Fig. 5A). Meanwhile, after incubation with 0.5, 5, and 50 μ mol/L SH1573, the protein binding rates of SH1573 in plasma of mice, rats, monkeys, and humans were all >99.5% (Fig. 5B). In addition, four metabolites of SH1573 can be seen in the liver microsomes of human, monkey, dog, rat and mouse, and all of them were products of oxidation (Fig. 5C). Therefore, SH1573 should be a medium-to high-permeability compound, which was expected to have considerable absorption *in vivo*.

3.6. SH1573 possessed high oral bioavailability and wide distribution *in vivo*

Next, the specific PK characteristics were explored in rats and monkeys. First, rats and monkeys were injected with 1 mg/kg SH1573 through the veins. The clearance rate was equivalent to 25.6% and 4.3% of liver blood flow, respectively. The elimination half-life was 16.3 and 12.2 h, and the steady-state distributed volume was 24.1 and 3.02 times the total liquid volume, respectively (Supporting Information Table S1). Importantly, with increasing dose, the absolute bioavailability in rats was 112.9%, 142.5% and 167.9% (Fig. 5D) and that of monkeys was 69.5%, 114% and 163% (Fig. 5E) according to Eq. (1):

$$\text{Absolute bioavailability (\%)} = \frac{(AUC_{i.g.} \times D_{i.v.})}{(AUC_{i.v.} \times D_{i.g.})} \times 100 \quad (1)$$

where D represents dosage. Moreover, the accumulation effect was studied. In rats, the peak concentration and the area under the curve from 0 to 24 h ($AUC_{0-24\text{ h}}$) of SH1573 obtained on Day 14 were 2.4 and 2.2 times those obtained on Day 1, respectively.

Since SH1573 had a long elimination half-life in rats, there was no significant accumulation of SH1573 in rats (Fig. 5F and Table S1). Meanwhile, in monkeys, the peak concentration on Day 14 was 5.0 times that on Day 1, and $AUC_{0-24\text{ h}}$ on Day 14 was 5.4 times that on Day 1, respectively. These findings show that after continuous dosing, SH1573 could accumulate in monkeys (Fig. 5F and Table S1). Finally, the tissue/plasma concentration ratio of SH1573 was analyzed in rats. SH1573 was detected in all tissues and was preferentially distributed in liver, fat, stomach, small intestine (duodenum), kidney and lung. Moreover, SH1573 could penetrate the blood–brain barrier, but that the intracerebral levels were approx. 15.65-fold lower than the levels in bone marrow (Fig. 5G). Briefly, we concluded that SH1573 displayed excellent absorption and tissue distribution with oral administration.

3.7. SH1573 mainly existed as a prototype and was excreted through faeces

To track its metabolic process *in vivo*, we used [¹⁴C] to mark SH1573³². After it was given to rats by gavage for 168 h, the accumulated excretion of radioactive substances in urine and faeces accounted for $98.0 \pm 1.7\%$, among which the radioactive substances in faeces accounted for $95.7 \pm 2.4\%$. The quality of radioactive material excreted in bile 48 h after administration accounted for $5.67 \pm 0.75\%$ of the dose, which showed that SH1573-related substances were mainly excreted through faeces (Fig. 5H). Meanwhile, during the excretion test, metabolites in plasma, urine, bile, and excrement homogenate of rats were identified. Sixteen metabolites were detected in addition to the original drugs. The main metabolic pathways of SH1573 in rats are mono-oxidation and glucuronic acid binding, and it is mainly excreted through faeces in the original form and as metabolites (Fig. 5I). A total of five metabolites were detected in the plasma of monkeys, of which the prototype was the main form (Fig. 5I). In summary, SH1573 existed stably and was excreted normally *in vivo*.

3.8. SH1573 displayed slight drug–drug interaction

In addition to the ADME process, it was important to find out whether SH1573 could influence the metabolism of other substances. First, an inhibitory test of the cytochrome P450 (CYP) enzyme showed that SH1573 had no inhibitory effect on CYP1A2, CYP2B6, CYP2D6, and CYP3A4, but had a moderate inhibitory effect on CYP2C8, CYP2C9, and CYP2C19 (Fig. 6A). Moreover, SH1573 had no induction effect on the enzyme activities of CYP1A2, CYP2B6, and CYP3A4 from three human primary liver cells (Fig. 6B). However, SH1573 at 10 μ mol/L had a potential induction effect on expression of *CYP2B6* in BXW cells, while it had a potential induction effect on expression of *CYP3A4* in all three liver cells (Fig. 6C). Meanwhile, SH1573 had stable metabolism in CYP1A2, CYP2B6, CYP2C8, CYP2C9, CYP2C19, CYP2D6, and CYP3A4 recombinant enzymes (Fig. 6D). Therefore, SH1573 interacted with CYPs slightly.

The following inhibitory test of transport showed that SH1573 had no significant inhibitory effect on the activity of MDR1. However, there was a concentration-dependent inhibitory effect on the activity of BCRP (Fig. 6E). Also, SH1573 had no obvious inhibitory effect on OATs and OCT2, but had a concentration-dependent inhibitory effect on OATPs (Fig. 6F). Finally, the uptake ratios of BCRP, MDR1, OATPs, OATs, and OCT2 to SH1573

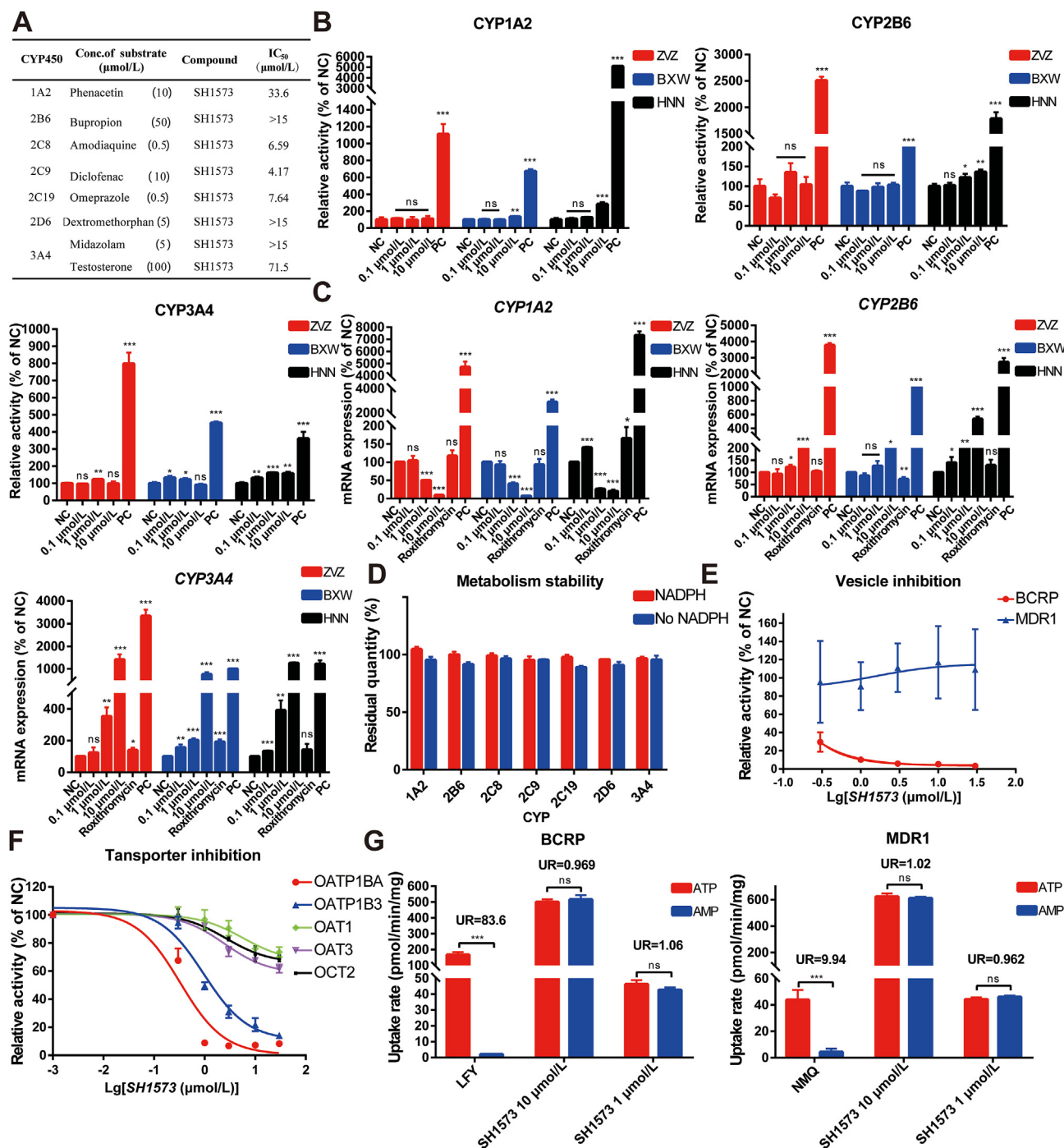


Figure 6 Drug interaction of SH1573. (A) The IC₅₀ of SH1573 to CYPs in human liver microsomes ($n = 2$). (B) and (C) The inducing effect of SH1573 on CYP1A2, CYP2B6 or CYP3A4 in ZVZ, BXW and HNN cell; NC: negative control; PC: positive control ($n = 3$). (D) The residual quantity of SH1573 after incubating with recombinant CYP enzymes for 60 min ($n = 3$). (E) The inhibitory effect of SH1573 to transport activity of BCRP and MDR1 ($n = 3$). (F) Inhibition effect of SH1573 on transport activity of OATPs, OATs and OCT2 ($n = 3$). (G) Uptake ratio of BCRP and MDR1 to SH1573; LFY: Lucifer yellow carbonylhydrazide; NMQ: *N*-methyl quinidine ($n = 3$). Data are expressed as mean (A) and mean \pm SD (B–G); *** $P < 0.001$, ns (no significant difference) versus NC group (B, C); *** $P < 0.001$, versus ATP group (G), ns: no significant difference.

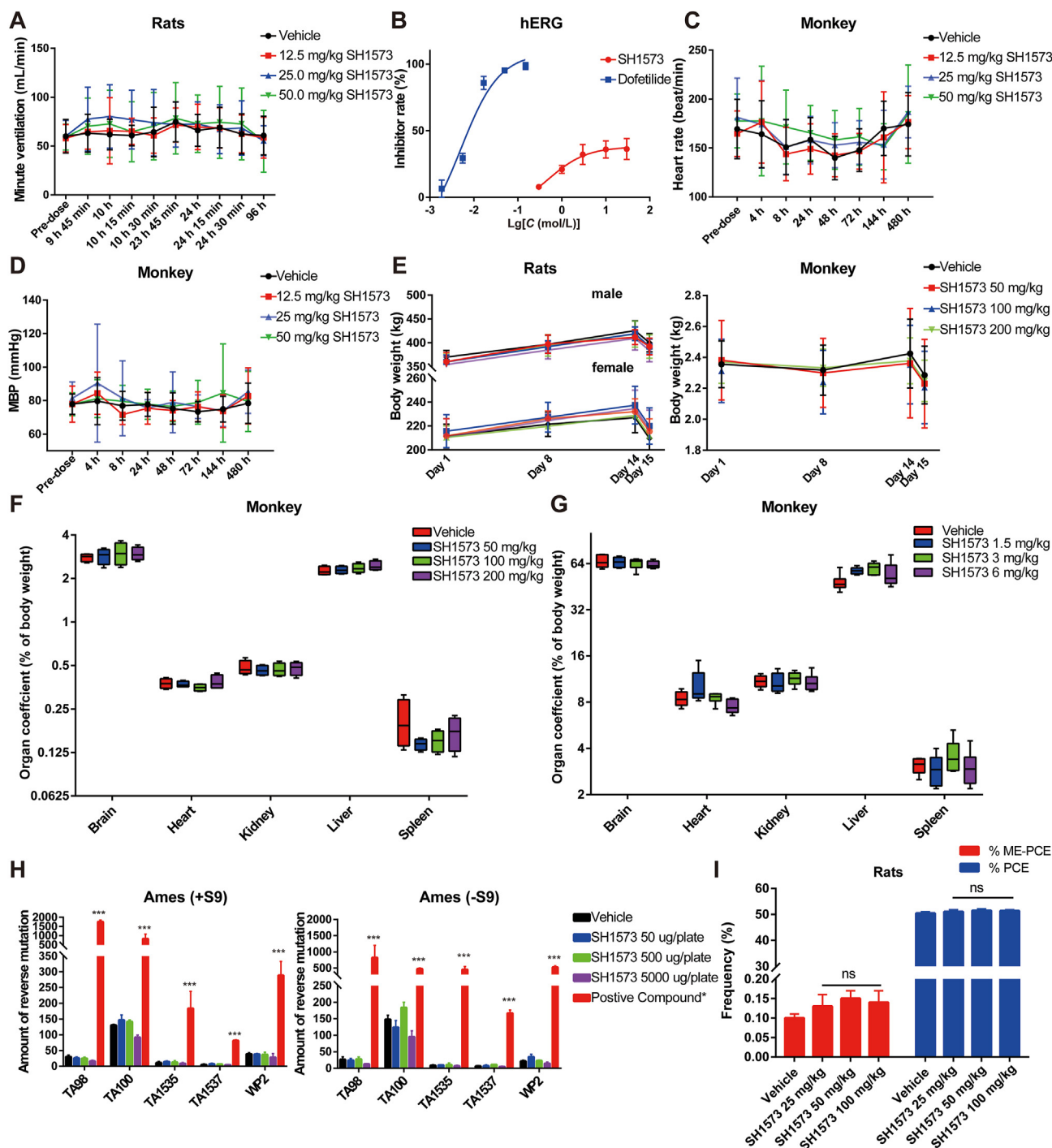


Figure 7 Toxicity evaluation of SH1573. (A) Rats were treated for once with vehicle i.g., 12.5 mg/kg SH1573 i.g., 25 mg/kg SH1573 i.g. or 50 mg/kg SH1573 and they minute ventilation was recorded for 96 h ($n = 16$). (B) The potassium channel inhibition rate ($n = 3$) of SH1573 on HEK293 cell expressed hERG. (C) and (D) Monkeys were treated for once with vehicle i.g., 12.5 mg/kg SH1573 i.g., 25 mg/kg SH1573 i.g. or 50 mg/kg SH1573. They heart rate and mean blood pressure (MBP) were record for 480 h ($n = 8$). (E) Rats were treated for once with vehicle i.g., 50 mg/kg SH1573 i.g., 100 mg/kg SH1573 i.g. or 200 mg/kg SH1573 and they body weight was recorded for 14 days ($n = 10$). (F) and (G) The body weight and organ coefficient of monkeys ($n = 4$) treated for once with vehicle i.g., 50 mg/kg SH1573 i.g., 100 mg/kg SH1573 i.g. or 200 mg/kg SH1573. The organ coefficient of monkeys ($n = 10$) treated for 28 days with vehicle i.g., 1.5 mg/kg SH1573 i.g., 3 mg/kg SH1573 i.g. or 6 mg/kg SH1573. i.g. (H) The amount of reverse mutaion in ames test ($n = 3$). (I) The micronucleus rate of rats in repeated administration toxicity test ($n = 3$). All data are expressed as mean \pm SD; *** $P < 0.001$ versus Vehicle QD group (H); ns: no significant difference versus Vehicle group (I).

were all lower than the baseline value (2.0), indicating that SH1573 was not the substrate of the above transporters^{33,34} (Fig. 6G and Supporting Information Fig. S2A). In short, SH1573 exhibited rare drug interaction effects.

3.9. SH1573 was safe for the respiratory, cardiovascular, and central nervous systems

In the final part of our study, the toxicological properties of SH1573 were analysed to guide future clinical trials. First, we found the respiratory (Fig. 7A, Fig. S2B and S2C) and central nervous systems (Supporting Information, Appendix C) were still not affected when the dose of SH1573 reached 50 mg/kg. Although SH1573 had a concentration-dependent inhibitory effect on the human Ether-à-go-go-Related Gene (hERG) potassium channels, the inhibition rate was less than 40% (Fig. 7B). In addition, after monkeys were given the highest dose of SH1573 (50 mg/kg) orally once, the electrocardiogram parameters (RR interval, PR interval, QRS interval, QT interval), heart rate, blood pressure and body temperature were not affected (Fig. 7C and D, Fig. S2D–S2G and Supporting Information, Appendix C). Thus, the no observed adverse effect level of SH1573 was 50 mg/kg for the respiratory, central nervous and cardiovascular systems. In other words, SH1573 was a fairly safe drug.

3.10. The reference dose of SH1573 for clinical trials was 6 mg/kg

After confirming that there were no serious side effects, we investigated the appropriate dosage for clinical administration. On the one hand, no related near-deaths or deaths occurred, and no abnormalities were observed in body weight, food intake, organ coefficient, gross autopsy, etc. when a single-dose of SH1573 reached 200 mg/kg (Fig. 7E and F; Supporting Information Fig. S3D and Appendix C). On the other hand, when SH1573 was given orally to rats once a day for 28 days, food intake in ≥ 100 mg/kg groups and weight gain (≥ 25 mg/kg groups) were decreased (Fig. S3A and S3B); five rats died (100 mg/kg group). Meanwhile, there were changes in organ coefficients, especially the liver (Fig. S3E). Importantly, after 28 days of administration, no deaths or near deaths occurred in monkeys. All doses of SH1573 caused a decrease in weight gain, while a weight decrease was observed in the 6 mg/kg group (Fig. S3C). We also found the organ coefficient of the liver increased slightly (≥ 1.5 mg/kg groups, Fig. 7G), while the volume and weight of the thymus decreased (≥ 3 mg/kg groups) (Supporting Information, Appendix C). However, all these adverse effects were reversed after stopping the drug. Therefore, with comprehensive consideration, we confirmed the reference dose for clinical trials was 6 mg/kg.

3.11. SH1573 was genetically safe

Finally, we performed the Ames test, cell micronucleus test, and chromosome aberration test to investigate the genotoxicity of SH1573^{35,36}. First, in the Ames test, no significant cytotoxicity was observed in all dose groups (5000, 500, and 50 μ g/plate) of SH1573 in all strains tested, with or without S9 mixture. Compared with the vehicle group, SH1573 did not induce ≥ 2 times (for TA98, TA100, and WP2uvrA) or ≥ 3 times (for TA1535 and TA1537) the average mutant colony number at all doses with or without S9 mixture, and no dose-dependence was found

(Fig. 7H). There was no significant change in the micronucleus rate compared with that of the vehicle control (Fig. 7I). Moreover, the chromosome aberration test showed that there was no significant increase in the percentage of chromosome structural aberration in each dose group compared with that in the vehicle group, indicating that SH1573 did not induce chromosome structural aberration³⁷ (Supporting Information Table S2). All the above data indicated that SH1573 did not have any genotoxicity.

4. Discussion

mIDH2, as an effective strategy for the treatment of AML, has received increasing attention from scientists and clinicians. Although AG-221 is the first mIDH2 inhibitor to be successfully marketed, potential drug resistance also makes the development of new mIDH2 inhibitors a promising effort³⁸. First, using computer aided drug design, we found that the active pocket binding to the labeled side of AG-221 can accommodate a larger structure. Thus, we designed SH1573 through ring transformation and found that it had better activity, selectivity and pharmacokinetic properties and successfully obtained related patents (CN109890806; CN107641114; WO2018014852). Interestingly, the binding site of AG-221 was located on the dimer interface³⁹, but the molecular docking results of SH1573 demonstrated that its binding site was not the same as AG-221, suggesting that SH1573 may act as a novel allosteric agent to inhibit the activity of mutant protein. Then, we verified its ability to inhibit mIDH2 R140Q *in vitro* using mIDH2 protein and mutant cell lines and evaluated its anti-tumor activity *in vivo* via CDX and PDX models. Moreover, the ADME progress and toxicological index of SH1573 were also evaluated in detail. As a result, our experiments have laid a solid foundation for the approval of a clinical trial (CTR20200247) and possible future marketing.

In fact, SH1573 had certain advantages compared to AG-221. Firstly, the binding site of AG-221 was on the interface, once Q316E and I319M mutations occurred, the binding capacity of AG-221 would be reduced, resulting in drug resistance³⁸. However, molecular simulation experiments showed that SH1573 was located at a possible allosteric site and did not bind to Q316 and I319, which was expected to solve the drug resistance problem of AG-221 (Fig. 1). Secondly, enzyme activity analysis showed that SH1573 had less impact on wtIDH1 and better inhibitory activity on R172K, which greatly increased the scope of its clinical application (Fig. 1). Meanwhile, SH1573 also had better pharmacodynamics efficacy than AG-221 *in vivo* (Fig. 4). It prolonged the survival time of PDX-bearing mice more significantly and better induce tumor cell differentiation. In addition, in terms of safety, SH1573 did not inhibit CYP2D6, P-gp, OAT1, OCT2 and MDR1, which reflected that SH1573 had fewer drug interactions than AG-221 (Fig. 6). Consequently, there could be a richer choice of drugs combination for SH1573. Therefore, it was these characteristics that made SH1573 smoothly enter phase I clinical trials.

Efficacy is a key evaluation index of new drug development. And experiments *in vitro* are the beginning and basis. In the part of enzyme and cell experiments, it showed that SH1573 had a weaker effect on wtIDH1 than AG-221 (Fig. 1G). Indeed, both SH1573 and AG-221 had strong selectivity. Their IC₅₀ for wtIDH1 far exceeded that for mIDH2 R40Q. Thus, with such a high selectivity, drugs that inhibited mIDH2 at concentrations will not affect wtIDH. Then, although the inhibitory effect of SH1573 on mIDH2 R140Q was similar as AG-221, SH1573 had better R172K

inhibitory activity and certain R172S inhibitory activity (Figs. 1E and 2B and Fig. S1E), which was of great help to its clinical applications. Despite SH1573 exhibits a certain pan-mIDH2 inhibitory activity, considering that 80% of patients with mIDH2 were R140Q mutation, we chose R140Q as the research focus, and we had conducted a comprehensive investigation in subsequent clinical trials. Meanwhile, the wild-type TF-1 contained 2-HG including (*S*)-2-HG and (*R*)-2-HG. It was reported that mIDH2 protein only produced (*R*)-2-HG, and (*S*)-2-HG recently found to be produced at high concentrations in renal cell cancer and in response to hypoxia⁴⁰. After SH1573 and AG-221 were applied to wild-type TF-1, it was found that the overall concentration of 2-HG did not change significantly, which partially reflected that mIDH2 inhibitors had no significant effect on the (*S*)-2-HG (Fig. 2A). After the mIDH2 R140Q protein was overexpressed into TF-1 cells, it was found that the concentration of 2-HG increased significantly (>10 fold). Therefore, it could be concluded from the above that the type of 2-HG inhibited by SH1573 was (*R*)-2-HG, at least most of which is (*R*)-2-HG. As previously reported, there were also some preclinical studies of mIDH2 inhibitor which use total 2-HG as the detection index^{41–43}, thus we will use (*R*)-2-HG in future experiments to get more accurate results. In brief, SH1573 did exhibit good efficacy *in vitro*, which made it worthy of further investigation.

Compared with cell and molecular biology experiments, experiments *in vivo* are the decisive factor for whether new drugs could enter the clinic. Although the effectiveness of SH1573 had been confirmed *via* the subcutaneous transplantation model (CDX, Fig. 3), considering that AML was a non-solid tumor, the intravenously injected PDX model could more realistically simulate the entire tumor process. Similar as AG-221, SH1573 increased the proportion of CD15⁺ cells in CD45⁺ cells (Fig. 4D). As a marker of leukocyte differentiation and maturation, increasing CD15⁺ cells marked the induction of differentiation⁴⁴, which was consistent with the previously reported mechanism of mIDH2 inhibitors. However, SH1573 also did not inhibit tumor proliferation as published reports of AG-221¹⁹. In fact, for hematological tumors, both killing tumor cells and inducing tumor cell differentiation could bring survival benefits to patients. Unlike cytotoxic drugs that could directly kill tumor cells to reduce tumor burden, the main efficacy of SH1573 and AG-221 were to reverse cell differentiation block, allowing tumor cells to differentiate normally and relieving hematopoietic dysfunction. At a dose of 45 mg/kg, both Ag-221 and SH1573 can significantly prolong the survival period of tumor-bearing mice, even SH1573 had a better effect (Fig. 4B). Moreover, it was noteworthy that SH1573 was better able to increase cell differentiation in the spleen of mice compared to AG-221, but the concentration of 2HG was similarly reduced when compared (Fig. 4D and E). As previously reported, AG-221 could induce cell differentiation independently of mIDH2⁴⁵. This was because that the ATP binding cassette subfamily G member 2 inhibition by AG-221 drove protoporphyrin IX accumulation, leading to increased heme and hemoglobin production in erythroid progenitors, thereby driving increased erythroid differentiation. We suspected that SH1573 could also induce cell differentiation independently with 2-HG, but related mechanisms were yet to be studied. In short, the experiment *in vivo* proved the better pharmacodynamic activity of SH1573.

As we all know, poor pharmacokinetic parameters often lead to failure of clinical trials, even new drugs with good pharmacodynamics^{46,47}. Fortunately, SH1573 performed well in series PK experiments as AG-221. Initially, in the part of

pharmacokinetics experiments *in vitro*, it showed that SH1573 exhibited fewer drug interactions. On the one hand, SH1573 did not inhibit CYP2D6, P-gp, OAT1 and OCT2 (Fig. 6A, E and F). It only slightly inhibited the activity of CYP2C8, CYP2C9 and CYP2C19 (Fig. 6A) and could increase the transcription levels of *CYP2B6* and *CYP3A4* (Fig. 6C), suggesting that attention should focus on these drugs metabolized by these enzymes in future drug combinations^{48,49}. On the other hand, BCRP and MDR1 were important efflux transporters to prevent effective accumulation of drugs in cells^{50,51}, but it was confirmed that SH1573 was not a substrate of these transporters (BCRP, MDR1, OATPs, OATs, and OCT2), indicating it could reach effective concentration in tumor cells⁵² (Fig. 6G). More importantly, AG-221 was a strong inhibitor of BCRP and MDR1⁵³, while SH1573 only inhibits BCRP. When patients use SH1573 in combination with substrates of BCRP (*e.g.*, methotrexate, imatinib, and topotecan), it may lead to drug accumulation in the cells, causing side effects. Therefore, we must pay attention to this point in possible future clinical applications. Moreover, well ADME characteristics *in vivo* were also the key to druggability. In this respect, compared to AG-221, SH1573 had similar characteristics⁵⁴. The difference between AG-221 and SH1573 in absorption was shown in the Supporting Information Table S3, which indicated that SH1573 might have better oral bioavailability. Interestingly, absolute bioavailability of SH1573 in rats was greater than 100% under three doses, which may be caused by the non-linear dynamic behaviour of SH1573 in rats (Fig. 5B). Then, AG-221 was mainly distributed in the stomach, liver, adrenal gland, harderian gland and brown adipose tissue. Similar as it, SH1573 was preferentially distributed in the liver, fat, stomach, small intestine (duodenum), kidney and lung (Fig. 5G). As for metabolism, oxidation and glucuronidation were the main metabolic pathway of AG-221 in rats, while that in humans was *N*-dealkylation⁵⁴. The metabolic pathway of SH1573 in rats was the same as AG-221, but its transformation in monkeys was mainly oxidation and acetylation (Fig. 5I). In addition, AG-221 and SH1573 were similar in excretion methods. Their prototype products and metabolites were mainly excreted in feces (>90%) in SD rats, and the prototype drugs in the excrement were all accounted for about 50% of the total drugs⁵⁴. This data suggest that AG-221 and SH1573 have approximately 50% absorption, and hepato-biliary excretion was the major elimination pathway in rats. Therefore, similar ADME features, better efficacy and better safety made SH1573 enter clinical trials successfully.

Currently, for the development of small molecule drugs, it is undoubtedly that the most innovative method is to design a compound with a new core according to the target, but it is also a successful strategy to modify the structure of existing drugs to achieve me-better effects. Such me-better drugs often have better druggability and shorter development cycles, which are a balanced expression of innovation and economy. Actually, SH1573 is the product of this method. Our research not only comprehensively evaluated SH1573, but also provided some ideas for the development and evaluation of subsequent mIDH2 inhibitors. However, there were still some problems to be solved urgently for SH1573. First and foremost, the specific sites of SH1573 binding to mIDH2 R140Q and the detailed mechanism of its pharmacological effects need to be explored later. Then, because the 28-day period of repeated administration was relatively short, the chronic toxicity of SH1573 needs to be evaluated. Finally, our study did not involve evaluation of reproductive toxicity, which needs to be explored in the future. Despite these shortcomings, our

experiments still confirmed that SH1573 has potential as an mIDH2 inhibitor.

5. Conclusions

In summary, we presented a preclinical assessment of the mIDH2 inhibitor SH1573 in AML. From our experiments, we confirm that not only does SH1573 possess strong inhibitory activity to mIDH2 R140Q *in vitro* or *in vivo* but also its ADME progress and safety are satisfactory. As a result, SH1573 has been approved for clinical trials in China. Collectively, this research contributed to the successful approval of SH1573 while providing a reference for future clinical trials. Importantly, we firmly believe that SH1573 will become another clinical mIDH2 inhibitor, bringing better treatment to AML patients.

Acknowledgments

This work was supported by National Key Research and Development Program of China (No. 2017YFA0205200), National Natural Science Foundation of China (Nos. 81773766 and 81903845), the Natural Science Foundation of Jiangsu Province (BK20161458, China) and the “Double First-Class” University project (No. CPU2018GY38, China).

Author contributions

Shengtao Yuan, Hongzhi Du and Meixiao Zhan contributed to the conception of the study and designed this experiment. Zhiqiang Wang, Zhibo Zhang and Yong Li performed the experiment and data analyses and wrote the manuscript. Li Sun, Dezheng Pen, Danyu Du, Xian Zhang, Luwei Han, Liwen Zhao and Ligong Lu helped perform the analysis with constructive discussions. All authors have read and agreed to the published version of the manuscript.

Conflicts of interest

The authors declare no conflict of interest.

Appendix A. Supporting information

Supporting data to this article can be found online at <https://doi.org/10.1016/j.apsb.2021.03.005>.

References

- Hanahan D, Weinberg RA. Hallmarks of cancer: the next generation. *Cell* 2011;**144**:646–74.
- Bader JE, Voss K, Rathmell JC. Targeting metabolism to improve the tumor microenvironment for cancer immunotherapy. *Mol Cell* 2020;**78**:1019–33.
- Vander Heiden MG, DeBerardinis RJ. Understanding the intersections between metabolism and cancer biology. *Cell* 2017;**168**:657–69.
- Deng H, Li W. Monoacylglycerol lipase inhibitors: modulators for lipid metabolism in cancer malignancy, neurological and metabolic disorders. *Acta Pharm Sin B* 2020;**10**:582–602.
- Stoddard BL, Dean A, Koshland Jr DE. Structure of isocitrate dehydrogenase with isocitrate, nicotinamide adenine dinucleotide phosphate, and calcium at 2.5-Å resolution: a pseudo-Michaelis ternary complex. *Biochemistry* 1993;**32**:9310–6.
- Waitkus MS, Diplas BH, Yan H. Biological role and therapeutic potential of *IDH* mutations in cancer. *Cancer Cell* 2018;**34**:186–95.
- Saha SK, Parachoniak CA, Bardeesy N. *IDH* mutations in liver cell plasticity and biliary cancer. *Cell Cycle* 2014;**13**:3176–82.
- Xu W, Yang H, Liu Y, Yang Y, Wang P, Kim SH, et al. Oncometabolite 2-hydroxyglutarate is a competitive inhibitor of α -ketoglutarate-dependent dioxygenases. *Cancer Cell* 2011;**19**:17–30.
- Ye D, Xiong Y, Guan KL. The mechanisms of *IDH* mutations in tumorigenesis. *Cell Res* 2012;**22**:1102–4.
- Lu C, Ward PS, Kapoor GS, Rohle D, Turcan S, Abdel-Wahab O, et al. *IDH* mutation impairs histone demethylation and results in a block to cell differentiation. *Nature* 2012;**483**:474–8.
- Marcucci G, Maharry K, Wu Y, Radmacher M, Mrózek K, Margeson D, et al. *IDH1* and *IDH2* gene mutations identify novel molecular subsets within *de novo* cytogenetically normal acute myeloid leukemia: a cancer and leukemia group B study. *J Clin Oncol* 2010;**28**:2348–55.
- Chou WC, Lei WC, Ko BS, Hou HA, Chen CY, Tang JL, et al. The prognostic impact and stability of isocitrate dehydrogenase 2 mutation in adult patients with acute myeloid leukemia. *Leukemia* 2011;**25**:246–53.
- Kats LM, Vervoort SJ, Cole R, Rogers AJ, Gregory GP, Vidacs E, et al. A pharmacogenomic approach validates AG-221 as an effective and on-target therapy in *IDH2* mutant AML. *Leukemia* 2017;**31**:1466–70.
- Boissel N, Nibourel O, Renneville A, Huchette P, Dombret H, Preudhomme C. Differential prognosis impact of *IDH2* mutations in cytogenetically normal acute myeloid leukemia. *Blood* 2011;**117**:3696–7.
- Green C, Evans C, Zhao L, Hills R, Burnett A, Linch D, et al. The prognostic significance of *IDH2* mutations in AML depends on the location of the mutation. *Blood* 2011;**118**:409–12.
- Nomdedéu J, Hoyos M, Carricondo M, Esteve J, Bussaglia E, Estivill C, et al. Adverse impact of *IDH1* and *IDH2* mutations in primary AML: experience of the Spanish CETLAM group. *Leuk Res* 2012;**36**:990–7.
- Fathi AT, Sadrzadeh H, Borger DR, Ballen KK, Amrein PC, Attar EC, et al. Prospective serial evaluation of 2-hydroxyglutarate, during treatment of newly diagnosed acute myeloid leukemia, to assess disease activity and therapeutic response. *Blood* 2012;**120**:4649–52.
- Losman JA, Loofer RE, Koivunen P, Lee S, Schneider RK, McMahon C, et al. (*R*)-2-Hydroxyglutarate is sufficient to promote leukemogenesis and its effects are reversible. *Science* 2013;**339**:1621–5.
- Yen K, Travins J, Wang F, David MD, Artin E, Straley K, et al. AG-221, a first-in-class therapy targeting acute myeloid leukemia harboring oncogenic *IDH2* mutations. *Cancer Discov* 2017;**7**:478–93.
- Stein EM, DiNardo CD, Pollyea DA, Fathi AT, Roboz GJ, Altman JK, et al. Enasidenib in mutant *IDH2* relapsed or refractory acute myeloid leukemia. *Blood* 2017;**130**:722–31.
- Stein EM. *IDH2* inhibition in AML: finally progress?. *Best Pract Res Clin Haematol* 2015;**28**:112–5.
- Garber K. First metabolic oncology inhibitor gets FDA green light, with record price tag. *Nat Biotechnol* 2017;**35**:895.
- Norsworthy KJ, Luo L, Hsu V, Gudi R, Dorff SE, Przepiorka D, et al. FDA approval summary: ivosidenib for relapsed or refractory acute myeloid leukemia with an isocitrate dehydrogenase-1 mutation. *Clin Cancer Res* 2019;**25**:3205–9.
- Boddu P, Borthakur G. Therapeutic targeting of isocitrate dehydrogenase mutant AML. *Expert Opin Invest Drugs* 2017;**26**:525–30.
- Camera A, Volpicelli M, Villa MR, Risitano AM, Rossi M, Rotoli B. Complete remission induced by high dose erythropoietin and granulocyte colony stimulating factor in acute erythroleukemia (AML-M6 with maturation). *Haematologica* 2002;**87**:1225–7.
- Chen J, Yang J, Wei Q, Weng L, Wu F, Shi Y, et al. Identification of a selective inhibitor of *IDH2/R140Q* enzyme that induces cellular differentiation in leukemia cells. *Cell Commun Signal* 2020;**18**:55.

27. Wunderlich M, Chou FS, Link KA, Mizukawa B, Perry RL, Carroll M, et al. AML xenograft efficiency is significantly improved in NOD/SCID-IL2RG mice constitutively expressing human SCF, GM-CSF and IL-3. *Leukemia* 2010;**24**:1785–8.
28. Her Z, Yong KSM, Paramasivam K, Tan WWS, Chan XY, Tan SY, et al. An improved pre-clinical patient-derived liquid xenograft mouse model for acute myeloid leukemia. *J Hematol Oncol* 2017;**10**:162.
29. Clement LT. Isoforms of the CD45 common leukocyte antigen family: markers for human T-cell differentiation. *J Clin Immunol* 1992;**12**:1–10.
30. Masungi C, Borremans C, Willems B, Mensch J, Van Dijck A, Augustijns P, et al. Usefulness of a novel Caco-2 cell perfusion system. I. *In vitro* prediction of the absorption potential of passively diffused compounds. *J Pharmacol Sci* 2004;**93**:2507–21.
31. Artursson P, Karlsson J. Correlation between oral drug absorption in humans and apparent drug permeability coefficients in human intestinal epithelial (Caco-2) cells. *Biochem Biophys Res Commun* 1991;**175**:880–5.
32. Clive S, Woo MM, Nydam T, Kelly L, Squier M, Kagan M. Characterizing the disposition, metabolism, and excretion of an orally active pan-deacetylase inhibitor, panobinostat, via trace radiolabeled ¹⁴C material in advanced cancer patients. *Cancer Chemother Pharmacol* 2012;**70**:513–22.
33. Xia CQ, Milton MN, Gan LS. Evaluation of drug–transporter interactions using *in vitro* and *in vivo* models. *Curr Drug Metabol* 2007;**8**:341–63.
34. Wang Z, Shang H, Li Y, Zhang C, Dong Y, Cui T, et al. Transporters (OATs and OATPs) contribute to illustrate the mechanism of medicinal compatibility of ingredients with different properties in yuan-huzhitong prescription. *Acta Pharm Sin B* 2020;**10**:1646–57.
35. Hayes AW, Hardisty JF, Harris SB, Weber K. The absence of genotoxicity of a novel fatty acid amide hydrolase inhibitor, BIA 10-2474. *Regul Toxicol Pharmacol* 2020;**111**:104556.
36. Kirkland DJ, Galloway SM, Sofuni T. International workshop on standardisation of genotoxicity test procedures. Summary of major conclusions. *Mutat Res* 1994;**312**:205–9.
37. Galloway SM. Chromosome aberrations induced *in vitro*: mechanisms, delayed expression, and intriguing questions. *Environ Mol Mutagen* 1994;**23 Suppl 24**:44–53.
38. Intlekofer AM, Shih AH, Wang B, Nazir A, Rustenburg AS, Albanese SK, et al. Acquired resistance to IDH inhibition through *trans* or *cis* dimer-interface mutations. *Nature* 2018;**559**:125–9.
39. Xie X, Baird D, Bowen K, Capka V, Chen J, Chenail G, et al. Allosteric mutant IDH1 inhibitors reveal mechanisms for *IDH1* mutant and isoform selectivity. *Structure* 2017;**25**:506–13.
40. Shelar S, Shim EH, Brinkley GJ, Kundu A, Carobbio F, Poston T, et al. Biochemical and epigenetic insights into L-2-hydroxyglutarate, a potential therapeutic target in renal cancer. *Clin Cancer Res* 2018;**24**:6433–46.
41. Gao M, Zhu H, Fu L, Li Y, Bao X, Fu H, et al. Pharmacological characterization of TQ05310, a potent inhibitor of isocitrate dehydrogenase 2 R140Q and R172K mutants. *Cancer Sci* 2019;**110**:3306–14.
42. Che J, Huang F, Zhang M, Xu G, Qu B, Gao J, et al. Structure-based design, synthesis and bioactivity evaluation of macrocyclic inhibitors of mutant isocitrate dehydrogenase 2 (IDH2) displaying activity in acute myeloid leukemia cells. *Eur J Med Chem* 2020;**203**:112491.
43. Nakagawa M, Nakatani F, Matsunaga H, Seki T, Endo M, Ogawara Y, et al. Selective inhibition of mutant IDH1 by DS-1001b ameliorates aberrant histone modifications and impairs tumor activity in chondrosarcoma. *Oncogene* 2019;**38**:6835–49.
44. Gadhoom SZ, Sackstein R. CD15 expression in human myeloid cell differentiation is regulated by sialidase activity. *Nat Chem Biol* 2008;**4**:751–7.
45. Dutta R, Zhang TY, Köhnke T, Thomas D, Linde M, Gars E, et al. Enasidenib drives human erythroid differentiation independently of isocitrate dehydrogenase 2. *J Clin Invest* 2020;**130**:1843–9.
46. Jang GR, Harris RZ, Lau DT. Pharmacokinetics and its role in small molecule drug discovery research. *Med Res Rev* 2001;**21**:382–96.
47. Li Y, Meng Q, Yang M, Liu D, Hou X, Tang L, et al. Current trends in drug metabolism and pharmacokinetics. *Acta Pharm Sin B* 2019;**9**:1113–44.
48. Mohamed MF, Jungerwirth S, Asatryan A, Jiang P, Othman AA. Assessment of effect of CYP3A inhibition, CYP induction, OATP1B inhibition, and high-fat meal on pharmacokinetics of the JAK1 inhibitor upadacitinib. *Br J Clin Pharmacol* 2017;**83**:2242–8.
49. Li XQ, Björkman A, Andersson TB, Gustafsson LL, Masimirembwa CM. Identification of human cytochrome P(450)s that metabolise anti-parasitic drugs and predictions of *in vivo* drug hepatic clearance from *in vitro* data. *Eur J Clin Pharmacol* 2003;**59**:429–42.
50. Wang J, Gan C, Retmana IA, Sparidans RW, Li W, Lebre MC, et al. P-glycoprotein (MDR1/ABCB1) and breast cancer resistance protein (BCRP/ABCG2) limit brain accumulation of the FLT3 inhibitor quizartinib in mice. *Int J Pharm* 2019;**556**:172–80.
51. Chen L, Manautou JE, Rasmussen TP, Zhong XB. Development of precision medicine approaches based on inter-individual variability of BCRP/ABCG2. *Acta Pharm Sin B* 2019;**9**:659–74.
52. Giacomini KM, Huang SM, Tweedie DJ, Benet LZ, Brouwer KL, Chu X, et al. Membrane transporters in drug development. *Nat Rev Drug Discov* 2010;**9**:215–36.
53. Megías-Vericat JE, Solana-Altabella A, Ballesta-López O, Martínez-Cuadrón D, Montesinos P. Drug–drug interactions of newly approved small molecule inhibitors for acute myeloid leukemia. *Ann Hematol* 2020;**99**:1989–2007.
54. Tong Z, Atsriku C, Yerramilli U, Wang X, Li Y, Reyes J, et al. Absorption, distribution, metabolism and excretion of an isocitrate dehydrogenase-2 inhibitor enasidenib in rats and humans. *Xenobiotica* 2019;**49**:200–10.